Interplay between Zonal Flows/GAMs and ITG Turbulence in Tokamak Plasmas

N. Miyato[1)], Y. Kishimoto[2),1)] and J. Q. Li[2)]

1) Japan Atomic Energy Agency, Naka, Ibaraki-ken, 311-0193, Japan
2) Graduate School of Energy Science, Kyoto University, Gokasho, Uji, Kyoto, 611-0011, Japan

e-mail: miyato.naoaki@jaea.go.jp

Abstract. Zonal flow behaviour and its effect on turbulent transport in tokamak plasmas are investigated by global fluid simulations of electrostatic ion temperature gradient (ITG) driven turbulence. It is found that oscillatory zonal flows called geodesic acoustic modes (GAMs) appearing in a high q (safety factor) region have the same frequency in a certain radial region whose width is almost proportional to $\sqrt{\rho_i a}$ in positive shear tokamaks, and the radial wavelength of the GAMs is proportional to ρ_i , where ρ_i is an ion Larmor radius and a is a minor radius of a plasma. The turbulent transport is affected by the nonlocal behaviour of the GAMs. It seems that the radial width of the region connecting a low tranport region where the stationary zonal flows are dominant with a high transport region where the GAMs are dominant is related with the nonlocal width of the GAMs. In reversed shear tokamaks, turbulent transport by the ITG turbulence is high in a broad radial region when the GAMs are dominant. The turbulent transport is reduced in a minimum q region where q is enough low to damp the GAMs. The difference of zonal flow behaviour causes the difference of the turbulent transport and may trigger formation of ion internal transport barriers in both positive and reversed shear tokamaks.

1 Introduction

Suppression of anomalous transport or formation of transport barriers is essential for confinement improvement of tokamak plasmas. Drift wave turbulence such as ion temperature gradient (ITG) driven turbulence is considered a cause of the anomalous transport and zonal flows generated from the drift wave turbulence regulate turbulent transport. This drift wave-zonal flow system has been studied by many authors extensively [1]. In recent years not a little theoretical and experimental attention has been devoted to geodesic acoustic mode (GAM) [2] which is a branch of zonal flows in toroidal plasmas. The GAM is oscillation of zonal flows due to coupling of the zonal flows with poloidally asymmetric (m, n)=($\pm$1, 0) pressure sidebands via geodesic curvature [3], where m and n are poloidal and toroidal mode numbers, respectively. Since the GAMs have finite frequency and are excited easily in a tokamak edge region with high safety factor (q), they are detected in many toroidal devices [4–12]. Recent nonlinear simulation studies have shown that geodesic transfer effect, which is energy transfer between the zonal flows and the pressure sidebands via the geodesic curvature, plays an important role in determining zonal flow level [3, 13–18]. Although conventional almost stationary zonal flows suppress the turbulent transport effectively, the GAMs are less effective in suppressing the turbulence because of their time varying nature [14, 18, 19]. Thus zonal flow behaviour including the GAMs may affect the anomalous transport and the formation of transport barriers in tokamak plasmas.

In this paper nonlinear interaction between the zonal flows/GAMs and the ITG turbulence in tokamak plasmas is studied by global ITG turbulence simulation. First we investigate effects of $\rho_* = \rho_i/a$ on the zonal flow behaviour and the turbulent transport in tokamak plasmas with positive magnetic shear, where ρ_i is an ion Larmor radius and a is a minor radius of a torus. Next the zonal flows/GAMs-ITG turbulence system in reversed shear tokamaks is analyzed. Finally results and conclusions are summarized.

2 Model Equations

A three-field electrostatic ion fluid model is used to describe the electrostatic ITG turbulence with adiabatic electrons. The model consists of an ion continuity equation,

$$\begin{aligned}\frac{dw}{dt} &= T_{eq}\frac{a}{n_{eq}}\frac{dn_{eq}}{dr}(1+\eta_i)\nabla_\theta\nabla_\perp^2\phi + \frac{a}{n_{eq}}\frac{dn_{eq}}{dr}\nabla_\theta\phi \\ &-\nabla_\parallel v_\parallel + \omega_d\cdot\left(\phi + T_i + \frac{T_{eq}}{n_{eq}}n\right) + D_w\nabla_\perp^2 w, \end{aligned} \tag{1}$$

an equation of motion for the ion fluid in the parallel direction,

$$\frac{dv_\parallel}{dt} = -\nabla_\parallel T_i - \frac{T_{eq}}{n_{eq}}\nabla_\parallel n - \nabla_\parallel\phi + D_v\nabla_\perp^2 v_\parallel, \tag{2}$$

an ion temperature equation with Hammett-Perkins closure [20],

$$\begin{aligned}\frac{dT_i}{dt} &= T_{eq}\frac{a}{n_{eq}}\frac{dn_{eq}}{dr}\eta_i\nabla_\theta\phi - (\Gamma-1)T_{eq}\nabla_\parallel v_\parallel - (\Gamma-1)\sqrt{\frac{8T_{eq}}{\pi}}|\nabla_\parallel|T_i \\ &+T_{eq}\omega_d\cdot\left((\Gamma-1)\phi + (2\Gamma-1)T_i + (\Gamma-1)\frac{T_{eq}}{n_{eq}}n\right) + D_T\nabla_\perp^2 T_i, \end{aligned} \tag{3}$$

and adiabatic response of electrons is given by,

$$n = \frac{n_{eq}}{\tau T_{eq}}(\phi - \langle\phi\rangle), \tag{4}$$

where, $w = n/n_{eq} - \nabla_\perp^2\phi$ is the generalized vorticity, n_{eq} (T_{eq}) is an equilibrium density (ion temperature) normalized by the central value n_c (T_c), $\tau = T_{e0}/T_{i0}$, $T_{e0}(T_{i0})$ is an electron (ion) equilibrium temperature, $\eta_i = d\ln T_{eq}/d\ln n_{eq}$, $\Gamma = 5/3$ is a ratio of specific heats and $\langle\cdot\rangle$ denotes the flux surface average. We assume circular tokamak geometry (r,θ,ζ), where r is a radius of magnetic surface, θ and ζ are poloidal and toroidal angles, respectively. Then operators are defined as

$$\frac{df}{dt} = \partial_t f + [\phi, f], \quad \omega_d\cdot f = 2\epsilon[r\cos\theta, f],$$

$$[f,g] = \frac{1}{r}\left(\frac{\partial f}{\partial r}\frac{\partial g}{\partial\theta} - \frac{\partial f}{\partial\theta}\frac{\partial g}{\partial r}\right),$$

where $\epsilon = a/R$ is an inverse aspect ratio, a and R are minor and major radii, respectively. Here the normalizations are $(tv_{ti}/a, r/\rho_i, \rho_i\nabla_\perp, a\nabla_\parallel) \rightarrow (t, r, \nabla_\perp, \nabla_\parallel)$,

$$\frac{a}{\rho_i}\left(\frac{n}{n_c}, \frac{e\phi}{T_c}, \frac{v_\parallel}{v_{ti}}, \frac{T_i}{T_c}\right) \rightarrow (n, \phi, v_\parallel, T_i)$$

where $v_{ti} = \sqrt{T_c/m_i}$, $\rho_i = v_{ti}/\omega_{ci}$, $\omega_{ci} = eB_0/m_i$. Artificial dissipations (D_w, D_v, D_T) are included to damp small scale fluctuations.

3 Effects of ρ_* on GAMs and Turbulent Transport in Positive Shear Tokamaks

In the previous work we reported that turbulent transort driven by the ITG turbulence can be controlled through the change of zonal flow behaviour by a q profile [14, 18]. However, it is difficult to connect the suppression of the turbulent transport by the stationary zonal flows with a transport barrier because radial variation of the transport obtained in the simulation is mild. This is due to large $\rho_* = \rho_i/a$ whose value used in the previous work is 0.0125. Global ITG turbulence simulations also showed that the frequency of the GAMs does not vary continuously with a radius, but its radial variation is step-like and frequency spectra of the GAMs have peaks at the same frequency in a certain radial region as shown in FIG. 1. In FIG. 1, the pure GAM frequency $f_{\rm GAM} = \sqrt{2(\Gamma+\tau)T_{eq}}(a/R)/2\pi$ and the pure parallel sound frequency of the (m,n)=(1, 0) mode $f_{\rm sound} = \sqrt{(\Gamma+\tau)T_{eq}}(a/qR)/2\pi$ are also plotted. This $f_{\rm sound}$ is typical frequency of dynamics along magnetic field for the (1, 0) mode in the model. When $f_{\rm sound}$ approaches the GAM frequencies, the GAMs will damp. The nonlocal behaviour in the GAM frequency was also observed experimentally in JFT-2M [21]. It is considered that the nonlocal behaviour becomes weak for small ρ_*.

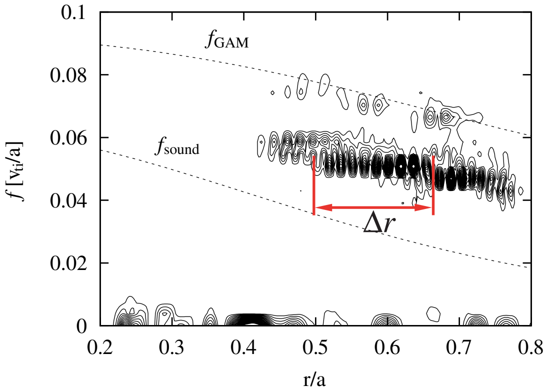

FIG. 1: Radial variation of zonal flow frequency spectra for $\rho_* = 0.005$. Frequency is normalized by v_{ti}/a. In the figure the pure GAM frequency $f_{\rm GAM} = \omega_{\rm GAM}/2\pi$ and the pure parallel sound wave frequency of the (1,0) mode $f_{\rm sound} = \omega_{\rm sound}/2\pi$ are also plotted.

We have performed global electrostatic ITG turbulence simulation with various ρ_* values from ρ_*=0.0125 to ρ_*=0.003, and investigated effects of ρ_* on the nonlocal behaviour of the GAMs and the turbulent transport. The other parameters used in the simulation are R/a=4, T_e=T_i, $n_{eq} = 0.8 + 0.2e^{-2(r/a)^2}$, $T_{eq} = 0.35 + 0.65(1-(r/a)^2)^2$, $q = 1.05 + 2(r/a)^2$. The temperature profile is fixed in the calculations. The numerical calculations are done by Fourier mode expansion in the poloidal and toroidal directions and finite difference in the radial direction. The Fourier modes included in the calculations are ones having resonant surfaces between $0.2 < r/a < 0.8$ with Δn=2, $n_{\rm max}$=50 for ρ_*=0.0125, Δn=4, $n_{\rm max}$=100 for ρ_*=0.005 and Δn=4, $n_{\rm max}$=124 for ρ_*=0.003, and nonresonant $(m,n) = (0,0),(1,0)$ components, where Δn is the interval of the toroidal mode number and $n_{\rm max}$ is the maximum toroidal mode number. The radial grid number is 256 for ρ_*=0.0125 and 512 for ρ_*=0.005 and 0.003. The artificial dissipations are set to $D_w = D_v = D_T = 4.8\times10^{-2}m^4(\rho_i/a)^3$. For the (0,0) mode, the dissipations are set to 10^{-4}.

The radial variation of zonal frequency spectra for ρ_*=0.005 is already shown in FIG. 1. When nonlinear terms are turned off artificially in a quasi steady state in the ρ_*=0.005 case, the GAMs become damped oscillations and their frequencies are near $f_{\rm GAM}$ as shown in FIG. 2. Hence, it is presumed that the turbulence is related with the nonlocal behaviour of the GAMs. It is found that the normalized radial width in which the GAMs have the same frequency, $\Delta r/a$, is almost proportional to $\sqrt{\rho_*}$, that is $\Delta r \propto \sqrt{\rho_i a}$, while the radial

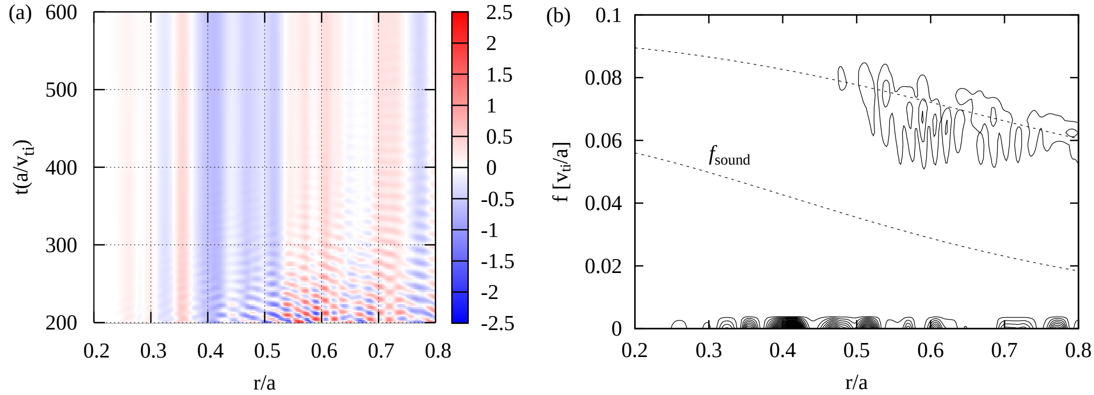

FIG. 2: (a) Zonal flows as a function of radius and time and (b) radial variation of zonal flow frequency spectra when nonlinear terms are turned off artificially in the $\rho_* = 0.005$ case.

wavelength of the GAMs is proportional to ρ_i [22]. Since the radial characteristic length of the linear toroidal ITG mode is also proportional to $\sqrt{\rho_i a}$, this result indicates that the radial structure of the GAMs in an ITG-GAM system is strongly affected by the toroidal ITG modes. Recently the eigenmode of GAM whose characteristic wavelength is $\rho_i^{2/3} L_T^{1/3}$ is obtained in the limit of $T_e \gg T_i$, where L_T is temperature scale length [23].

Figure 3 shows radial variations of ion thermal diffuisivity χ normalized by $\rho_i^2 v_{ti}/a$ and zonal flow frequency spectra for three different cases. The zonal flow frquency spectra and the χ profiles denoted by a solid line are obtained from the simulation with only (0, 0) and (1, 0) modes for $n = 0$. The χ profiles denoted by a dashed line are obtained from the simulation with more $n = 0$ modes up to (m, n)=(9, 0). It is noted that the region where strong GAMs are excited is mainly determined by the pressure and the safety factor

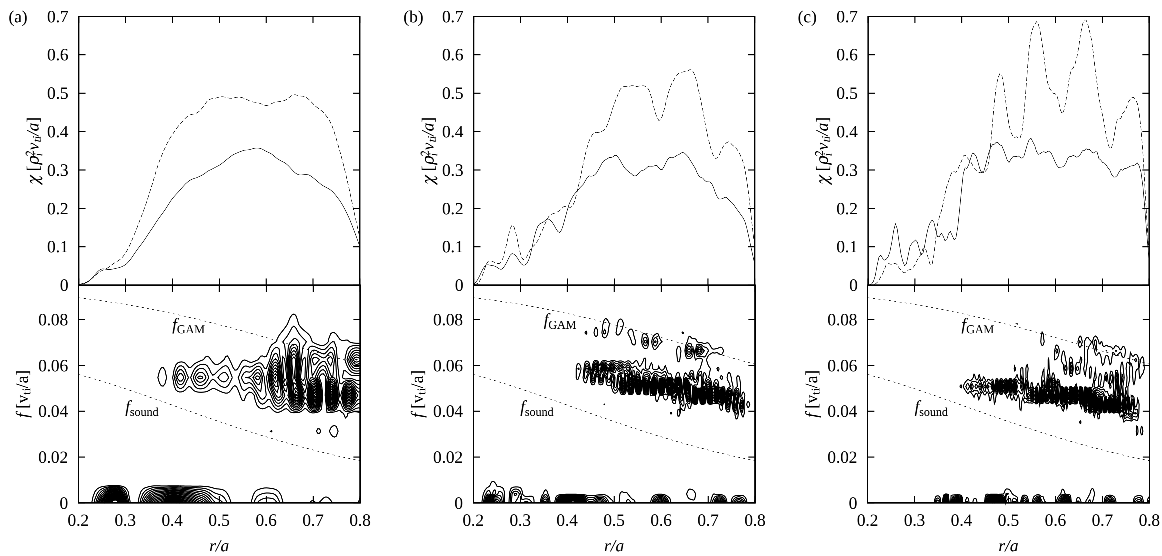

FIG. 3: Radial variations of normalized ion thermal diffusivity and zonal flow frequency spectra for (a) $\rho_* = 0.0125$, (b) $\rho_* = 0.005$ and (c) $\rho_* = 0.003$. The zonal flow frquency spectra and the χ profiles denoted by a solid line are obtained from the simulation with only (0, 0) and (1, 0) modes for $n = 0$. The χ profiles denoted by a dashed line are obtained from the simulation with more $n = 0$ modes up to (m, n)=(9, 0).

profiles and almost independent of ρ_*. Since the GAM frequencies are close to those of the ITG turbulence, the GAM dominant region ($r/a > 0.4$) is a high transport region and the statinoary zonal flow region ($r/a < 0.4$) is a low transport region in general. It is expected in a local sense that χ varies rapidly around $r/a = 0.4$ where is the boundary between the GAMs and the stationary zonal flows. However the GAMs have the nonlocal nature whose characteristic length is Δr and the turbulent transport is affected by the nonlocal behaviour of the GAMs. It seems that the radial width of the region connecting the low tranport region with the high transport one is related with the nonlocal width of the GAMs, Δr. In the $\rho_* = 0.0125$ case, the slope of χ beginning around $r/a = 0.3$ goes up to $r/a \approx 0.6$ and it is difficult to recognize the boundary between the low and the high transport regions. The gradient of χ around $r/a = 0.4$ is steeper for smaller ρ_* and the radial width of the connection region decreases with ρ_*. The boundary between the low and the high transport regions is very clear in the $\rho_* = 0.003$ case. The difference of χ between the low and the high transport regions increases when the more $n = 0$ modes are included in the simulation. In the case with the more $n = 0$ modes, the (1, 0) pressure perturbation energy is partly transferred to the higher m and $n = 0$ modes and the GAMs become weak. On the other hand, the inclusion of the more $n = 0$ modes does not affect the stationary zonal flows strongly. As a consequence, the turbulent transport in the GAM region in the case with the more $n = 0$ modes is higher than that in the case with only (0, 0) and (1, 0) modes as shown in FIG. 3.

4 Numerical Results in Reversed Shear Tokamaks

In this section we report results of the ITG turbulence simulation in tokamak plasmas with the reversed magnetic shear configuration. We have performed the simulation with the q profiles shown in FIG. 4(a) for $\rho_* = 0.005$. The other parameters are the same as the positive shear case. It is noted that for the reversed shear cases several nonresonant modes of $n \neq 0$ are included in the calculation in addition to the modes having resonant surfaces between $0.2 < r/a < 0.9$ and the nonresonant (m, n)=(0, 0), (1, 0) modes. Since global gyrokinetic analyses showed that ITG modes in reversed shear tokamaks have finite nonresonant components whose ratio m/n is close to $q_{\min}$ [24, 25], nonresonant modes of $n \neq 0$ should be included. Effect of the nonresonant modes on a linear eigenfunction of the ITG mode in a reversed shear tokamak is shown in FIG. 5. In the case with nonresonant modes (FIG. 5(a)), a slab-like structure appears on a minimum q surface [24,26], but such a structure is not seen in the case without nonresonant modes (FIG. 5(b)).

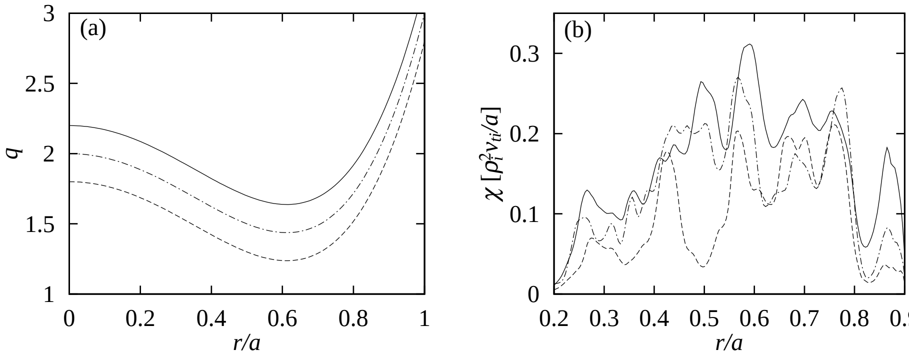

FIG. 4: Radial profiles of (a) safety factor q and (b) normalized ion thermal diffusivity for $q = 2.2-3(r/a)^2+4(r/a)^4$ (solid), $q = 2-3(r/a)^2+4(r/a)^4$ (dash dot) and $q = 1.8-3(r/a)^2+4(r/a)^4$ (dash).

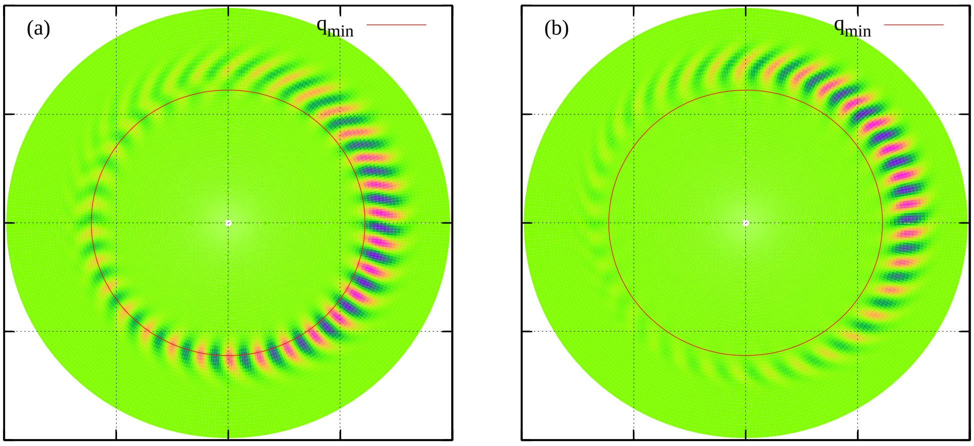

FIG. 5: Eigenfunctions of the ITG mode with $n = 22$ in a reversed shear plasma in the case (a) with and (b) without nonresonant modes for q=$2 - 3(r/a)^2 + 4(r/a)^4$ and $\rho_* = 0.0125$.

Figure 4(b) shows radial variations of normalized ion thermal diffusivity χ for the q profiles shown in FIG. 4(a). In the high q case (solid line in FIG. 4), the ion turbulent heat transport is high in a broad region, because the GAMs are dominant in almost the whole region as shown in FIG. 6(a). Decrease of the transport is not seen in a minimum q region where an internal transport barrier (ITB) has been observed in several tokamak experiments [27]. In the low q case (dashed line in FIG. 4), however, the turbulent transport is reduced around $r/a = 0.5$. This is due to change of zonal flow behaviour. As shown in FIG. 6, the parallel sound frequency $f_{\rm sound}$ approaches the frequencies of the GAMs and the GAMs damp, when q is reduced. In the region where the GAMs are alive, the turbulent transport is still high. Here it is noted that the turbulent transport around the radius of maximum $f_{\rm sound}$ ($r/a \approx 0.515$) is more reduced than that around a minimum q surface ($r/a \approx 0.612$). This point is not clear in the previous simulation for $\rho_* = 0.0125$ [28]. If more $n = 0$ modes were included as in the positive shear cases, the gap of the turbulent transport would be deeper.

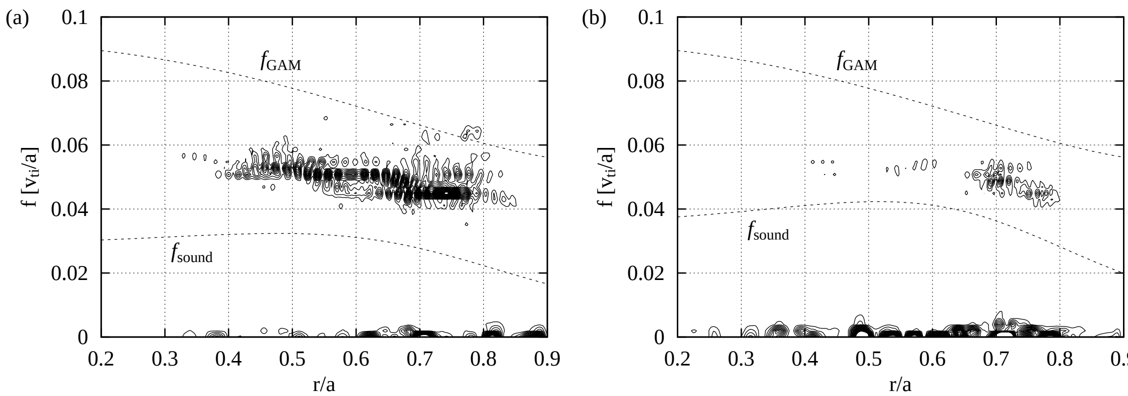

FIG. 6: Radial variation of zonal flow frequency spectra for (a) $q = 2.2 - 3(r/a)^2 + 4(r/a)^4$ and (b) $q = 1.8 - 3(r/a)^2 + 4(r/a)^4$.

5 Summary and Conclusions

We have performed electrostatic ITG turbulence simulations in both positive and reversed shear tokamaks. It is found that in the positive shear tokamaks the radial width in which GAMs have the same frequency, Δr, is almost proportional to $\sqrt{\rho_i a}$ and this nonlocal behaviour of the GAMs may arise from combination of the GAMs and the ITG turbulence. Besides it seems that the radial width of the region connecting a low tranport region where stationary zonal flows are dominant with a high transport region where the GAMs are dominant is related with the nonlocal width of the GAMs. The boundary between the low and high transport regions is clearer for smaller ρ_*. When more $n = 0$ modes are included in the calculations, the GAMs are weakened by energy transfer to higher m modes and the difference of χ between the low and high transport regions expands. In the reversed shear tokamak with low q, reduction of turbulent transport has been observed around the radius of maximum $f_{\rm sound}$ near a minimum q surface where the stationary zonal flows are excited. On the other hand, there is no reduction of the turbulent transport in the minimum q region in the high q case because the GAMs are dominant. Thus the difference of zonal flow behaviour causes the difference of the turbulent transport and may trigger formation of ion ITBs in both positive and reversed shear tokamaks. In order to simulate the ITB formation to the final stage, it is necessary to include other effects such as heating and equiribrium E×B flow driven neoclassically. Simulation of the ITG turbulence driven by heating is in progress. The results of the simulation with $\rho_* = 0.0125$ have shown that central temperature is the highest in the case of the reversed shear plasma with low q when heat source is fixed. The simulation with smaller ρ_* and inclusion of the E×B flow will be done in a future study.

The authors would like to thank Dr. T. Ido, Dr. M. Yagi, Dr. A. Ishizawa, Dr. Y. Idomura, Dr. T. Matsumoto and Dr. Y. Ishii for useful discussions. We also thank Dr. M. Kikuchi and Dr. H. Ninomiya for their support. This work is partly supported by Grant-in-Aid from the Japan Society for the Promotion of Science (No. 18760646).

References

[1] DIAMOND, P. H., et al., Plasma Phys. Control. Fusion **47**, R35 (2005).

[2] WINSOR, N., JOHNSON, J. L., and DAWSON, J. M., Phys. Fluids **11**, 2448 (1968).

[3] HALLATSCHEK, K., and BISKAMP, D., Phys. Rev. Lett. **86**, 1223 (2001).

[4] SHATS, M. G., and SOLOMON, W. M., Phys. Rev. Lett. **88** 045001 (2002).

[5] SCHOCH, P. M., et al., Rev. Sci. Instrum. **74**, 1846 (2003).

[6] MCKEE, G. R., et al., Phys. Plasmas **10**, 1712 (2003).

[7] FUJISAWA, A., et al., Phys. Rev. Lett. **93**, 165002 (2004).

[8] HAMADA, Y., et al., Nucl. Fusion **45**, 81 (2005).

[9] CONWAY, G. D., et al., Plasma Phys. Control. Fusion **47**, 1165 (2005).

[10] IDO, T., et al., Nucl. Fusion **46**, 512 (2006).

[11] MELNIKOV, A. V., et al., Plasma Phys. Control. Fusion **48**, S87 (2006).

[12] KRÄMER-FLECKEN, A., et al., Phys. Rev. Lett. **97**, 045006 (2006).

[13] SCOTT, B., Phys. Lett. A **320**, 53 (2003).

[14] MIYATO, N., KISHIMOTO, Y. and LI, J. Q., Phys. Plasmas **11**, 5557 (2004).

[15] SCOTT, B. D., New J. Phys. **7**, 92 (2005).

[16] NAULIN, V., et al., Phys. Plasmas **12**, 052515 (2005).

[17] KENDL, A. and SCOTT, B. D., Phys. Plasmas **12**, 064506 (2005).

[18] MIYATO, N., LI, J. Q. and KISHIMOTO, Y., Nucl. Fusion **45**, 425 (2005).

[19] HAHM, T. S., et al., Phys. Plasmas **6**, 922 (1999).

[20] HAMMETT, G. W. and PERKINS, F. W., Phys. Rev. Lett. **64**, 3019 (1990).

[21] IDO, T., et al., Plasma Phys. Control. Fusion **48**, S41 (2006).

[22] MIYATO, N., KISHIMOTO, Y. and LI, J. Q., Plasma Phys. Control. Fusion **48**, A335 (2006).

[23] ITOH, K., et al., Plasma Fusion Res. **1**, 037 (2006).

[24] IDOMURA, Y, TOKUDA, S. and KISHIMOTO, Y., Nucl. Fusion **43**, 234 (2003).

[25] CANDY, J., WALTZ, R. E. and ROSENBLUTH, M. N., Phys. Plasmas **11**, 1879 (2004).

[26] LI, J. Q., et al., Phys. Lett. A **233**, 85 (1997).

[27] CONNOR, J. W., et al., Nucl. Fusion **44**, R1 (2004).

[28] MIYATO, N., LI, J. Q. and KISHIMOTO, Y., to be published in J. Plasma Phys.